Supplementary Information (SI) for Polymer Chemistry.

# Supporting Information

# Carboxylic acid α-end functionalized poly(2-oxazoline)s synthesized through benzylic CROP initiators

*Caroline T. Holick, Nora Engel, Nicole Fritz, Christine Weber, Ulrich S. Schubert**

Caroline T. Holick, Nora Engel, Nicole Fritz, Christine Weber, Ulrich S. Schubert
Laboratory of Organic and Macromolecular Chemistry (IOMC), Friedrich Schiller University Jena, Humboldtstrasse 10, 07743 Jena, Germany
Email: ulrich.schubert@uni-jena.de

Caroline T. Holick, Nora Engel, Nicole Fritz, Christine Weber, Ulrich S. Schubert
Jena Center for Soft Matter (JCSM), Friedrich Schiller University Jena, Philosophenweg 7, 07743 Jena, Germany

Ulrich S. Schubert
Helmholtz Institute for Polymers in Energy Applications Jena (HIPOLE Jena), Lessingstraße 12–14, 07743 Jena, Germany

Ulrich S. Schubert
Helmholtz-Zentrum Berlin für Materialien und Energie GmbH (HZB), Hahn-Meitner-Platz 1, 14109 Berlin, Germany

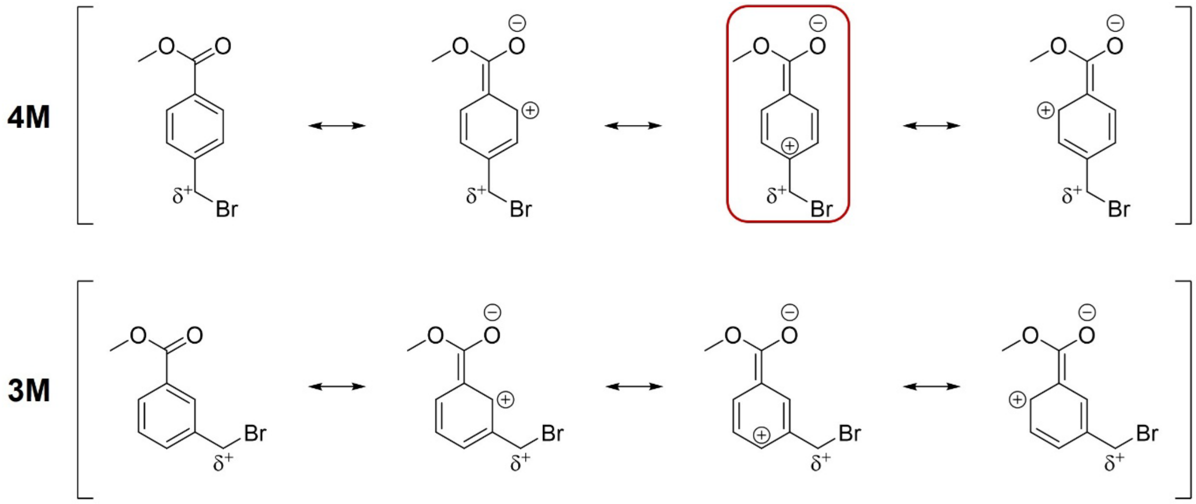

**Scheme S1**: Schematic representation of the resonance structures for methyl 4-(bromomethyl)benzoate (**4M**) and methyl 3-(bromomethyl)benzoate (**3M**).

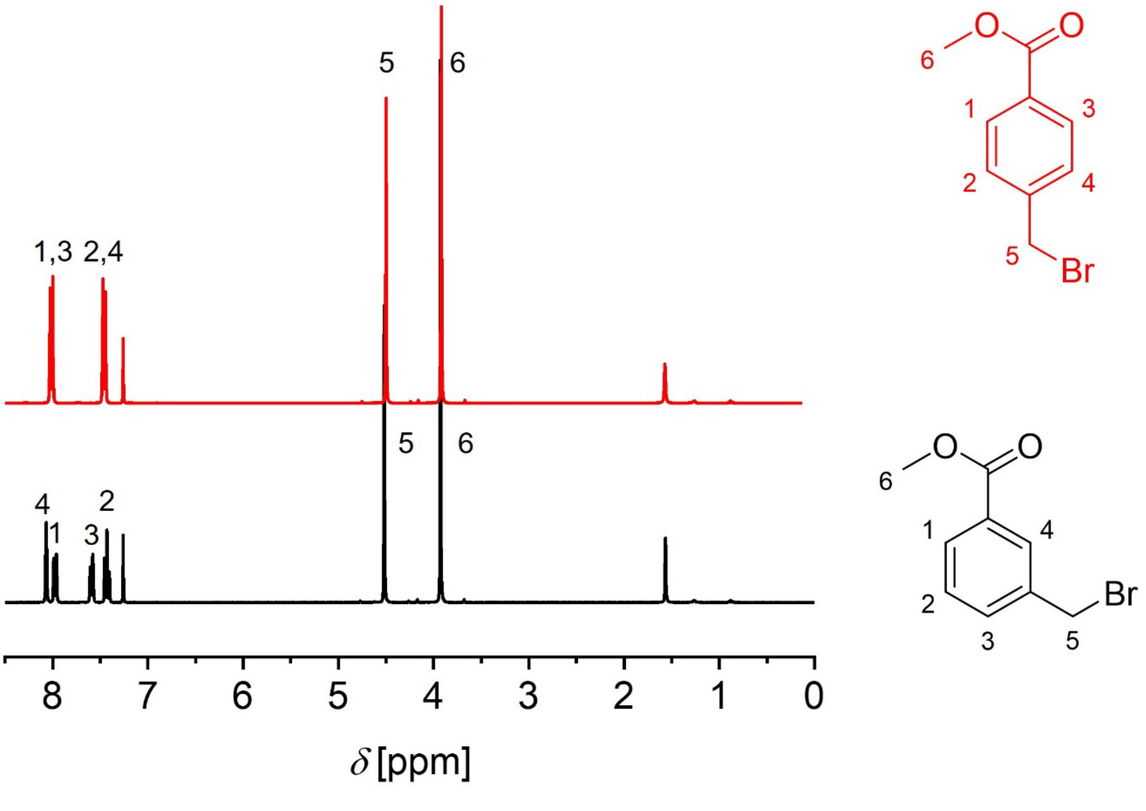

**Figure S1**: $^1$H NMR spectra of methyl-4-(bromomethyl)benzoate (**4M**, red) and methyl-3-(bromomethyl)benzoate (**3M**, black).

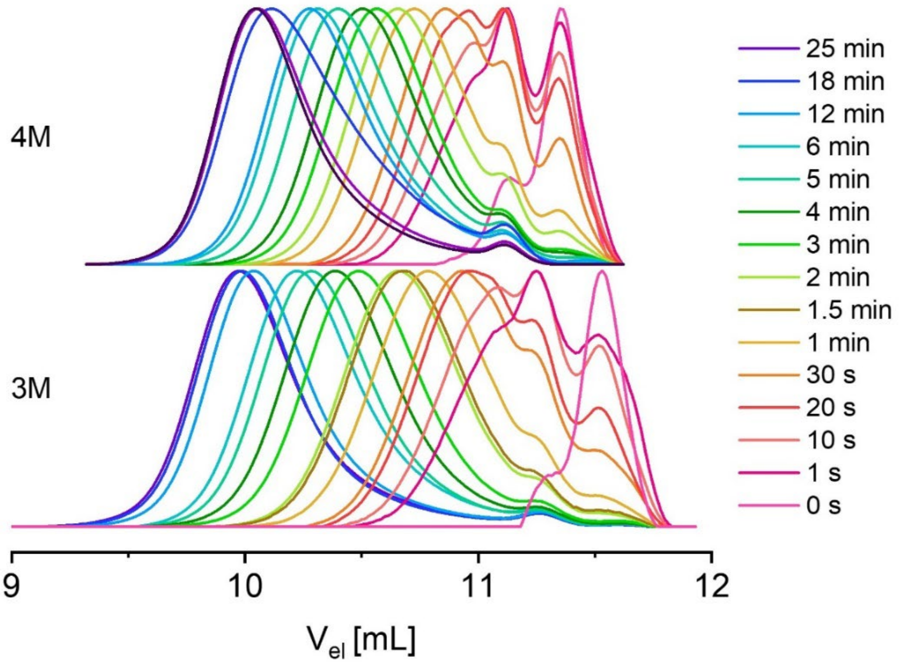

**Figure S2**: Overlay of the SEC elugrams (RID) taken during the CROP of EtOx initiated by **3M** or **4M** at 140 °C.

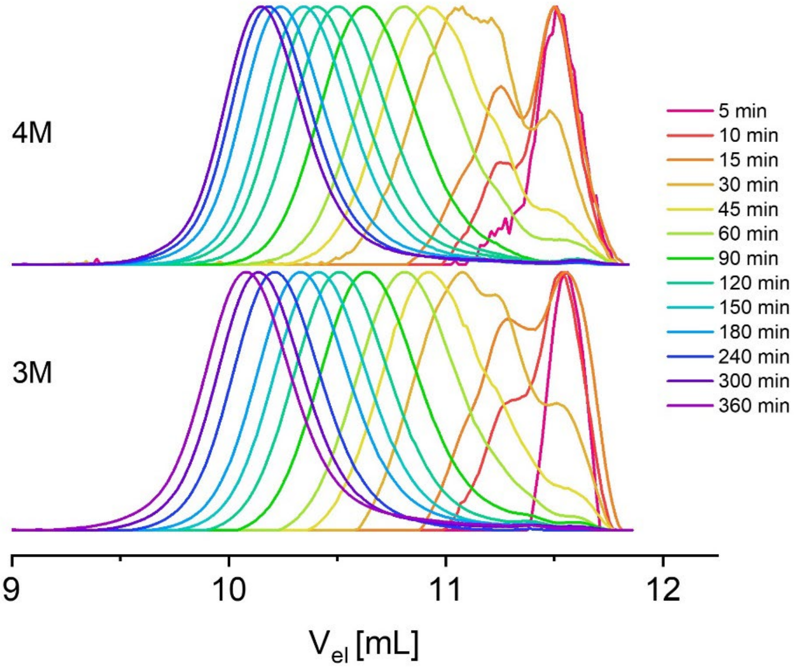

**Figure S3**: Overlay of the SEC elugrams (RID) taken during the CROP of EtOx initiated by **3M** or **4M** at 85 °C.

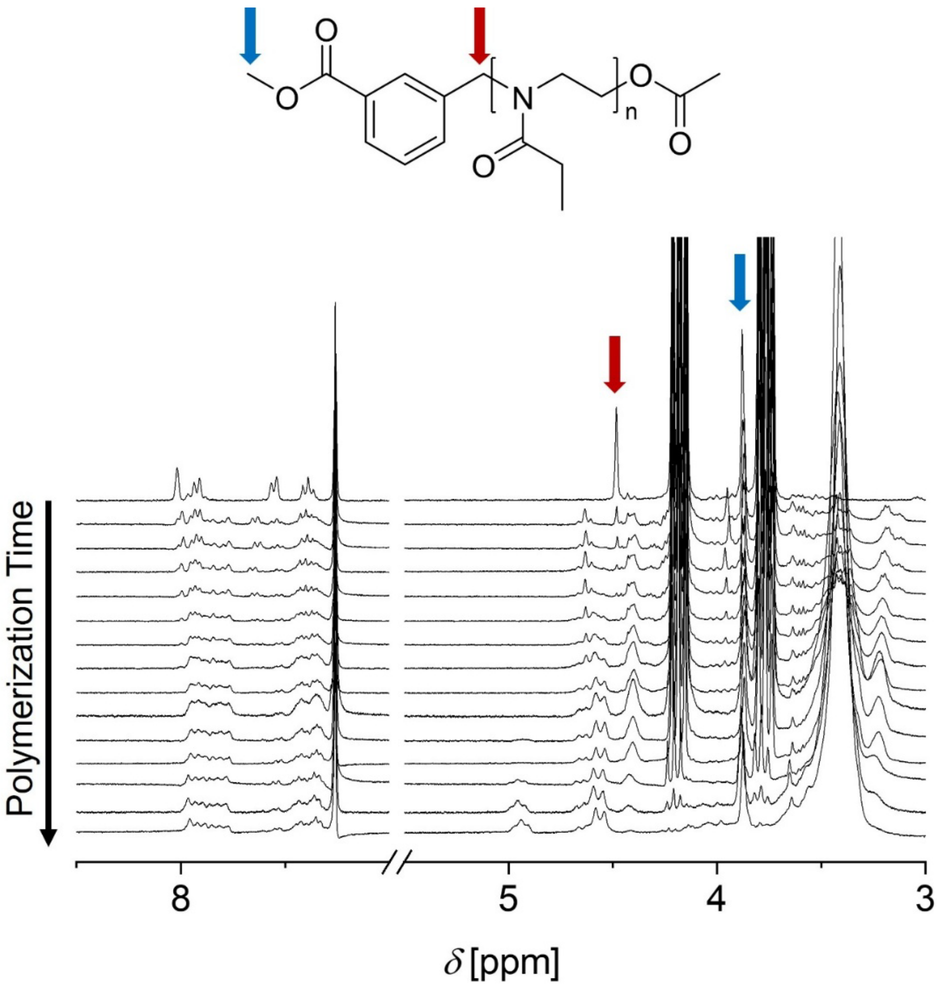

**Figure S4**: Overlay of $^1$H NMR spectra taken during the CROP of EtOx initiated by **3M** at 140 °C. Arrows indicate the proton signals used to determine the initiation efficiency.

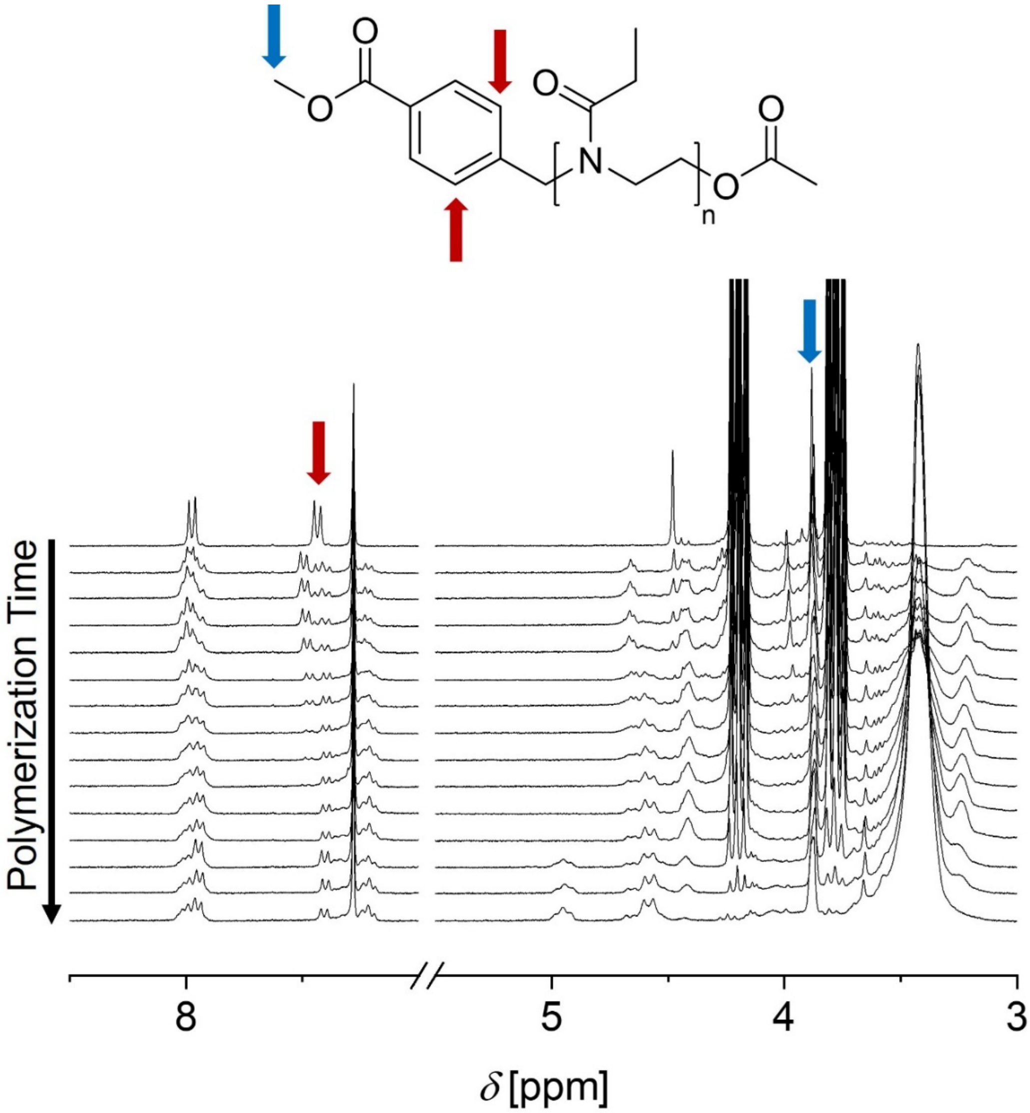

**Figure S5**: Overlay of $^1$H NMR spectra during the CROP of EtOx initiated by **4M** at 140 °C. Arrows indicate the protons used to determine the initiation efficiency.

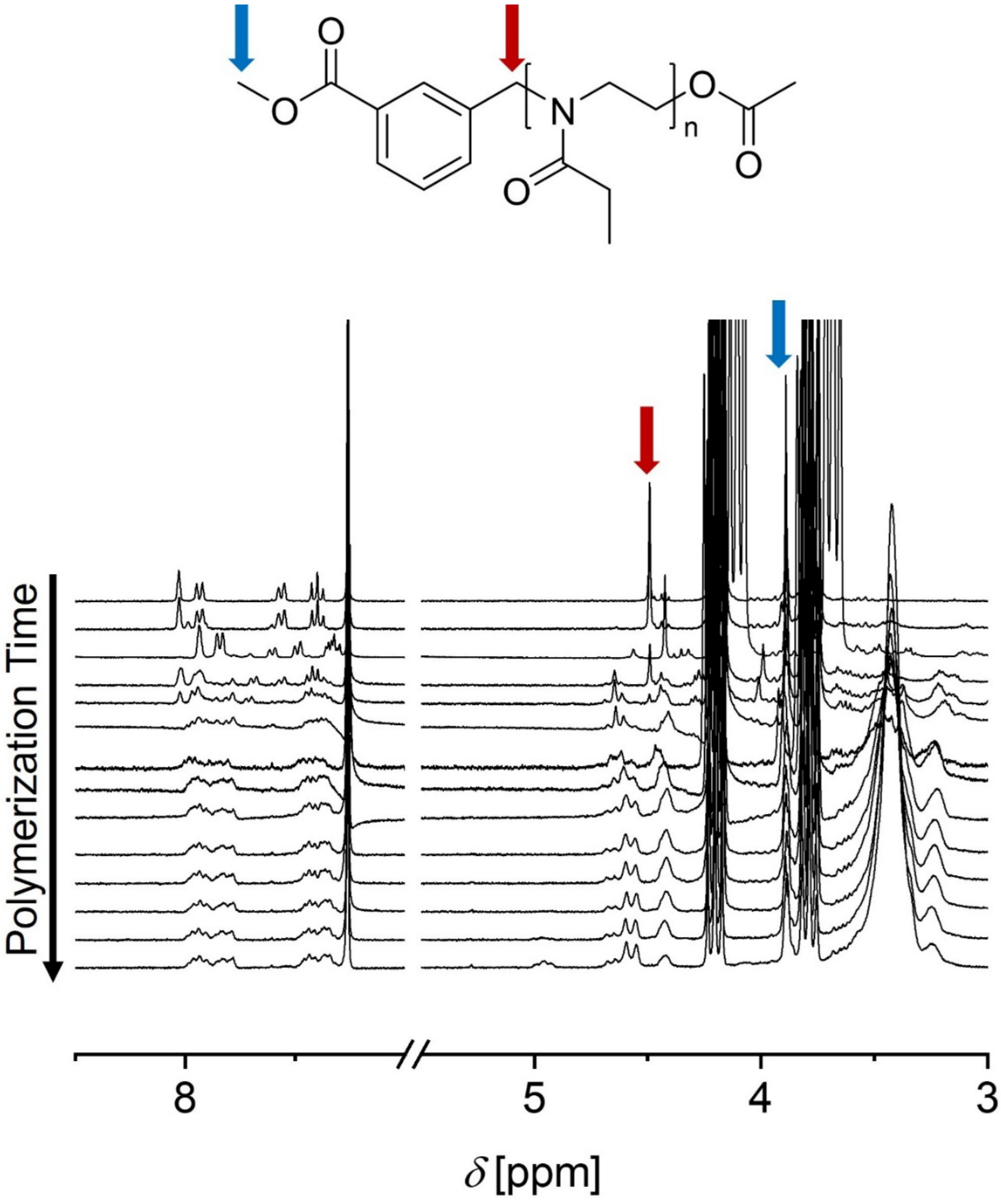

**Figure S6**: Overlay of $^{1}$H NMR spectra during the CROP of EtOx initiated by **3M** at 85 °C. Arrows indicate the protons used to determine the initiation efficiency.

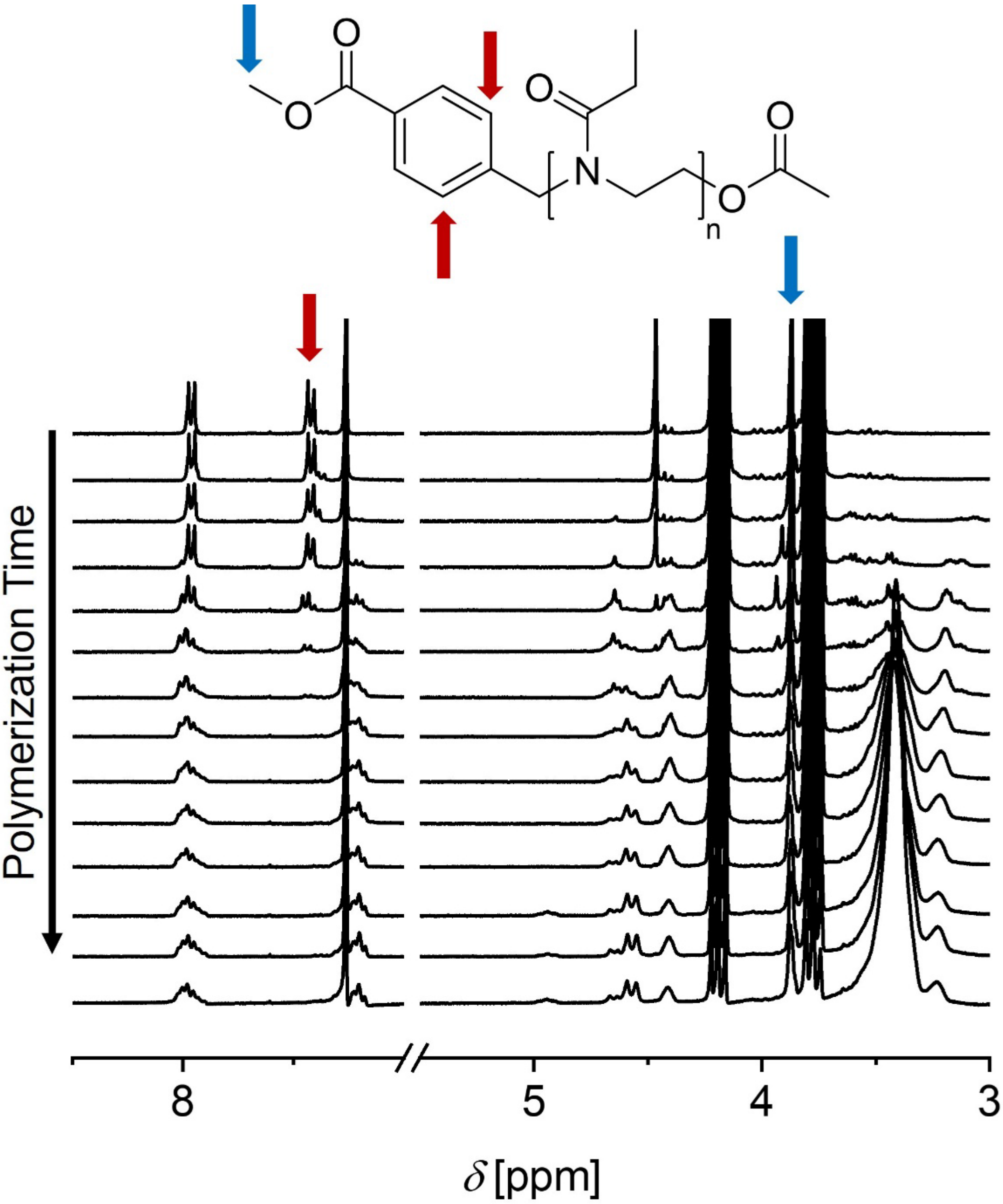

**Figure S7**: Overlay of $^1$H NMR spectra during the CROP of EtOx initiated by **4M** at 85 °C. Arrows indicate the protons used to determine the initiation efficiency.

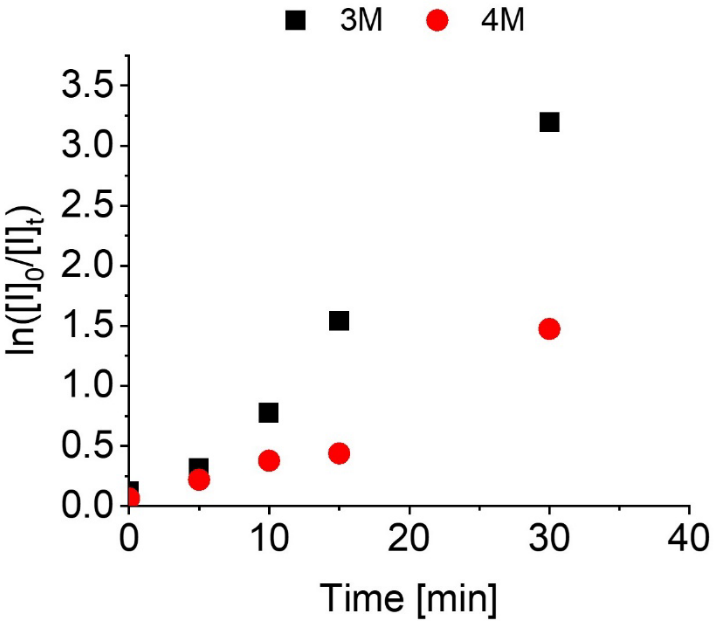

**Figure S8**: First order kinetic plot regarding initiator concentration during the during the CROP of EtOx initiated by **3M** or **3M** at 85 °C. [I]$_0$/[I]$_t$ was estimated from the $^1$H NMR spectra.

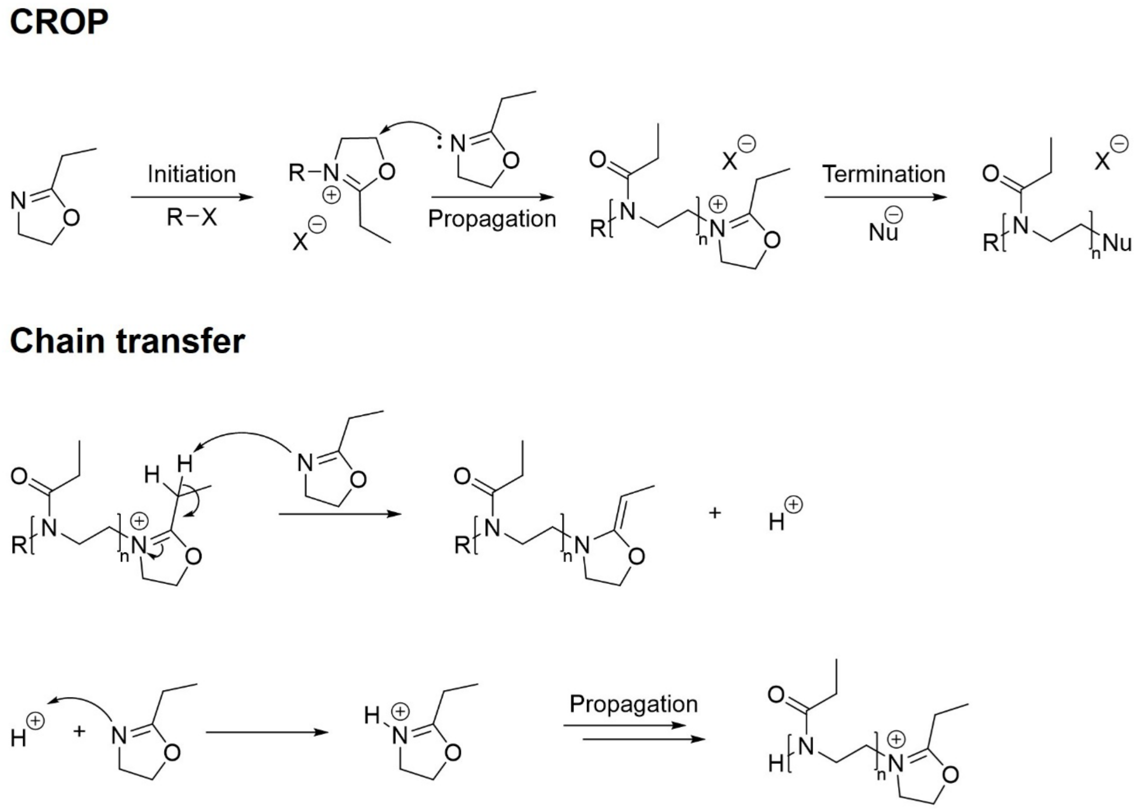

**Scheme S2**: Schematic representation of the cationic ring-opening polymerization and chain transfer reaction.

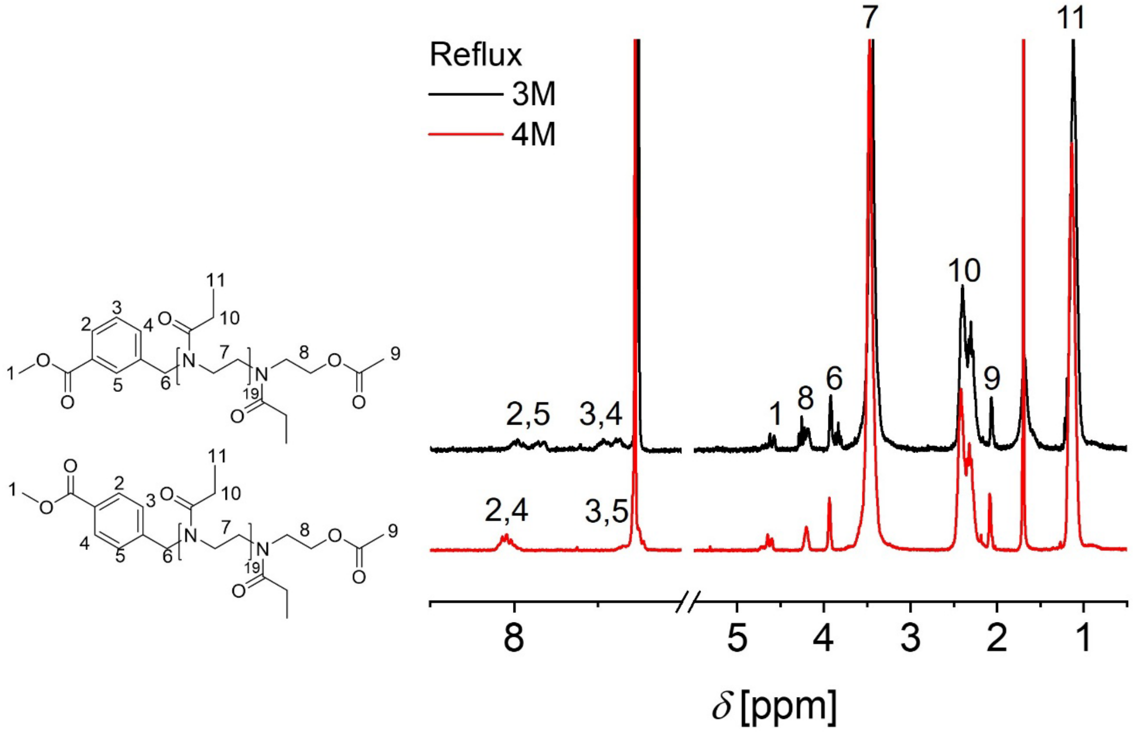

**Figure S9**: $^1$H NMR spectra (300 MHz, CDCl$_3$) of **3M-EtOx$_{20}$-OAc** and **4M-EtOx$_{20}$-OAc** synthesized under reflux conditions (85 °C) including assignments of the peaks to the schematic representation of the structures.

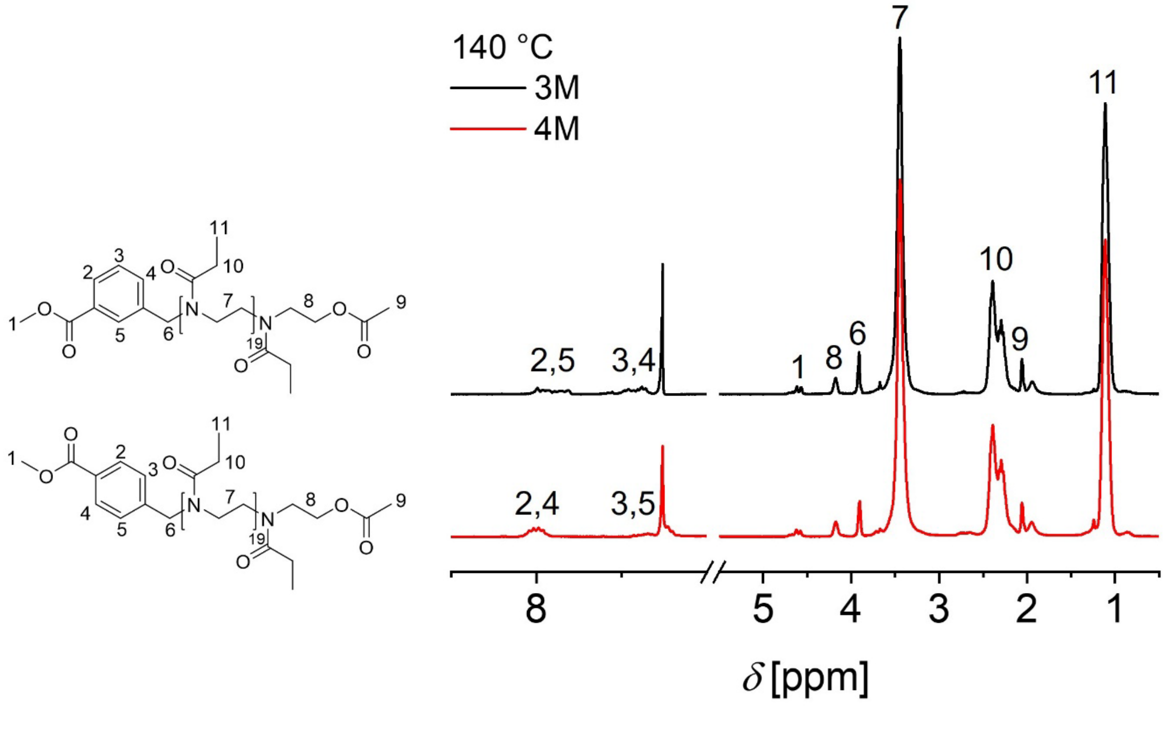

**Figure S10**: $^1$H NMR spectra (300 MHz, CDCl$_3$) of **3M-EtOx$_{20}$-OAc** and **4M-EtOx$_{20}$-OAc** synthesized at 140 °C including assignments of the peaks to the schematic representation of the structures.

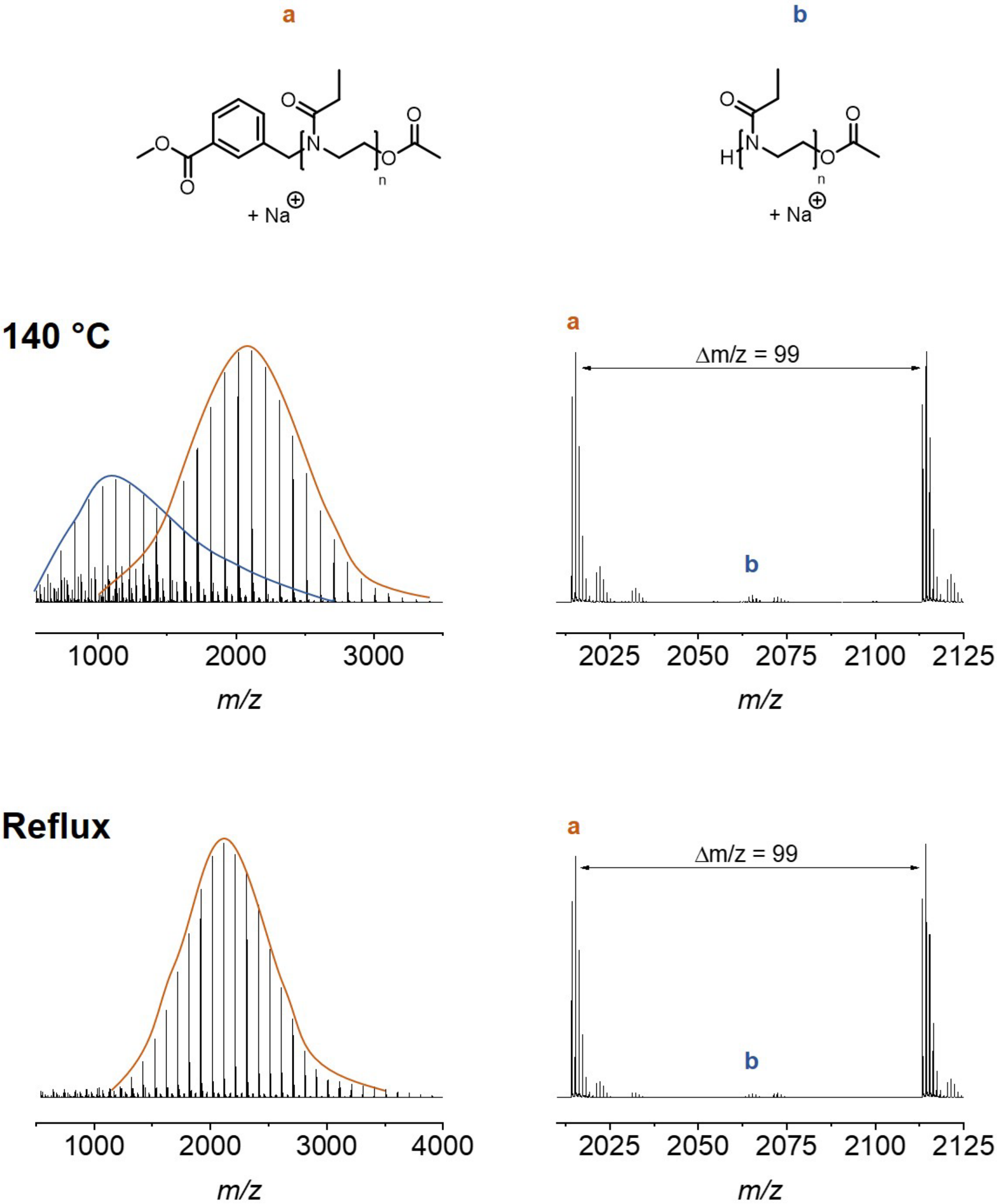

**Figure S11:** MALDI-TOF MS measurements of **3M-EtOx$_{20}$OAc** synthesized under reflux conditions (85 °C) or at 140 °C. Left: Full spectra. Right: Zoom into the most abundant *m/z* region to display the EtOx repeating unit of Δ*m/z* = 99 and peak assignment.

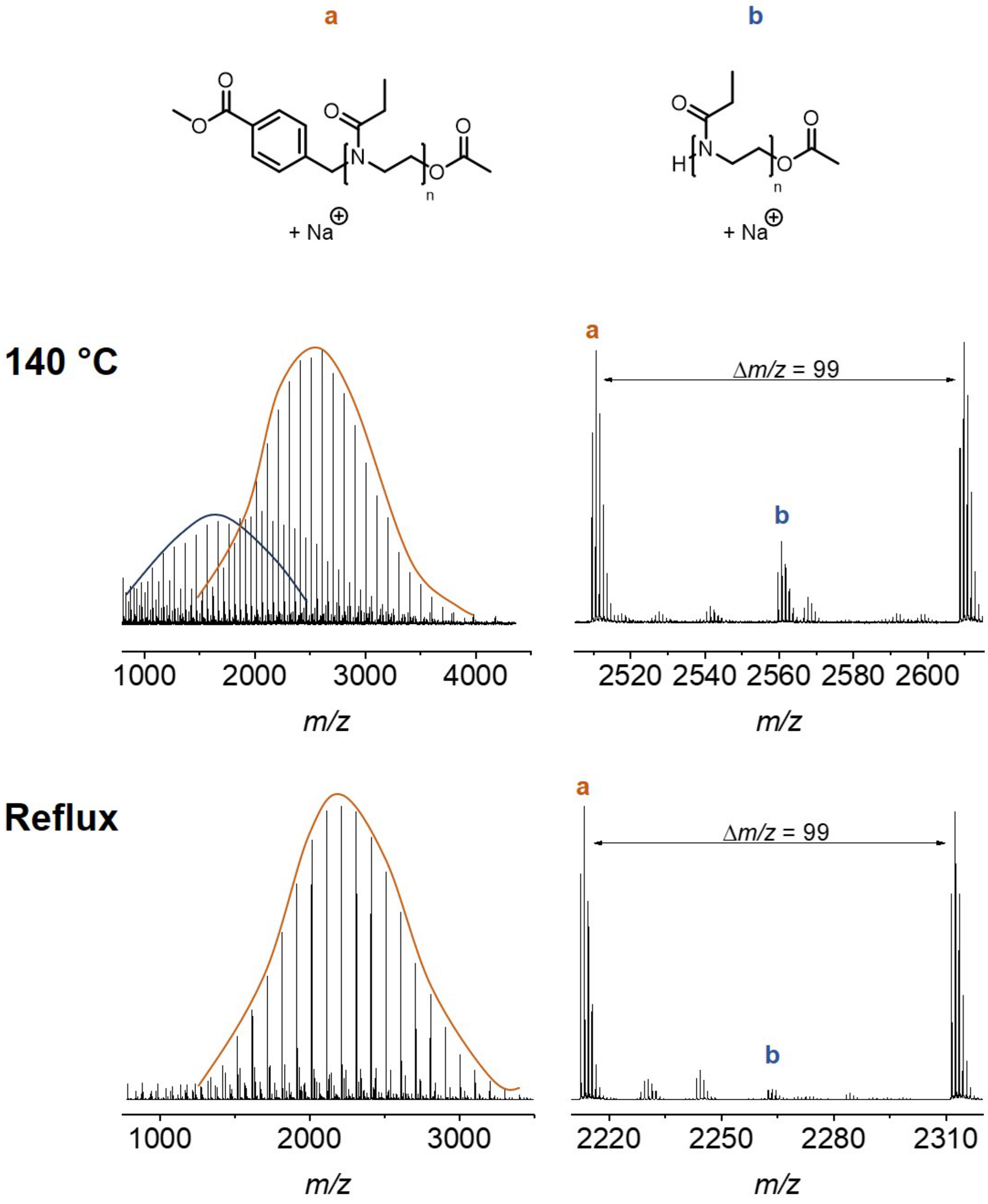

**Figure S12**: MALDI-TOF MS measurements of **4M-EtOx$_{20}$OAc** synthesized under reflux conditions (85 °C) or at 140 °C. Left: Full spectra. Right: Zoom into the most abundant *m/z* region to display the EtOx repeating unit of Δ*m/z* = 99 and peak assignment.

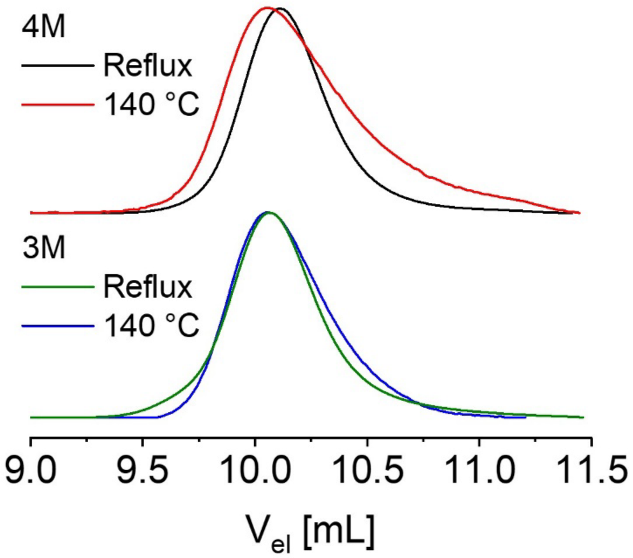

**Figure S13**: SEC elugrams (RI detection) of **3M-EtOx$_{20}$-OAc** and **4M-EtOx$_{20}$-OAc** synthesized at 140 °C or under reflux conditions (85 °C).

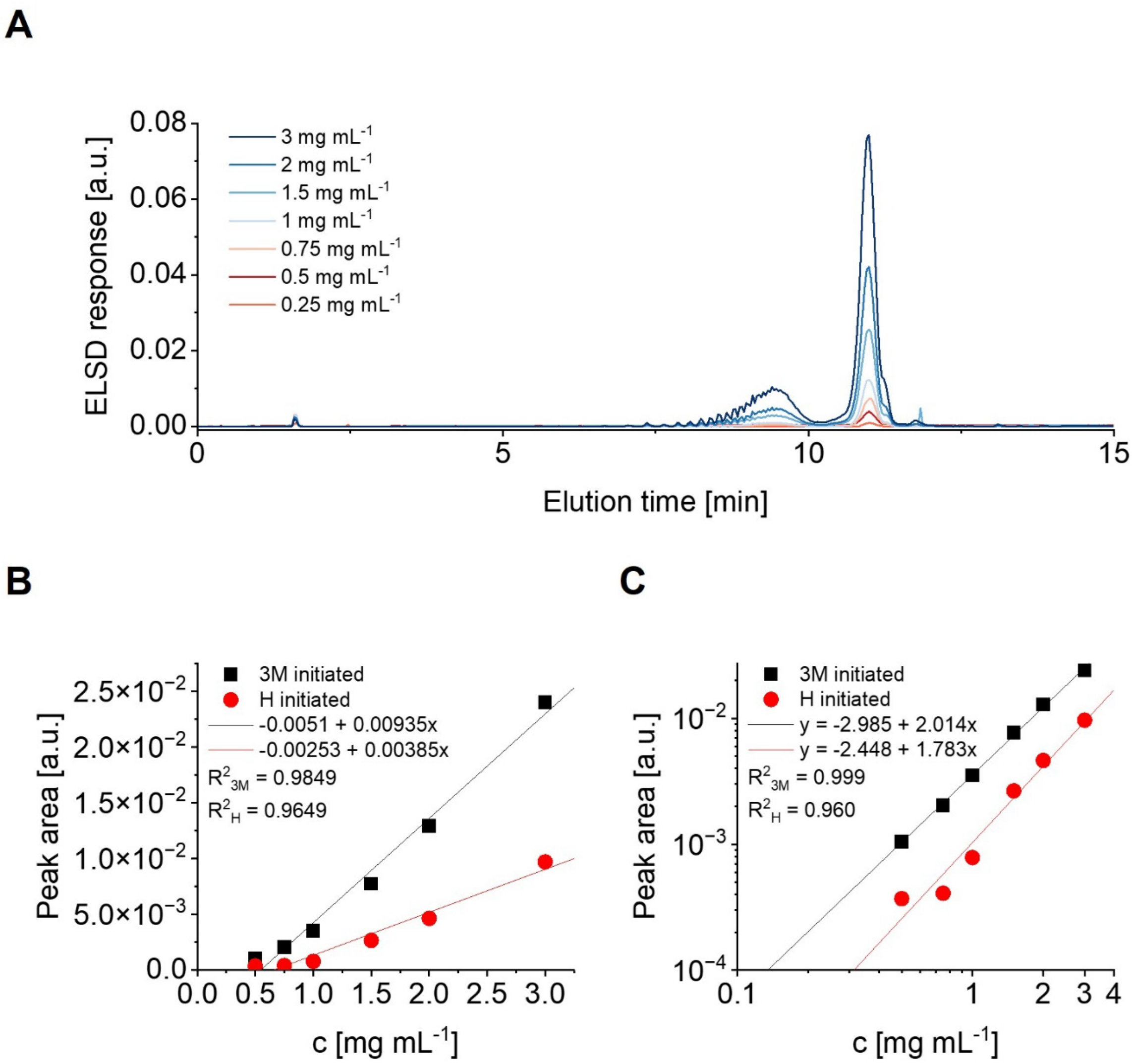

**Figure S14**: ELSD linearity test using a serial dilution of **4M-EtOx$_{20}$-OAc**. **A**: Elugrams of all measured concentrations. **B** Plot of signal area for the signal at around 10.9 min (**4M** initiated) and 9.5 mL (H initiated) against polymer concentration. **C**: Double logarithmic plot of signal area for the signal at around 10.9 min (**4M** initiated) and 9.5 mL (H-initiated) against polymer concentration.

**Table S1**: Signal area percentages from the HPLC chromatograms of **4M-EtOx$_{20}$-OAc** (synthesized at 140 °C) measured at varying concentrations.

| **Concentration** <br> **[mg mL$^{-1}$]** | **Signal area$_{\text{4M initiated}}$** <br> **[%]** | **Signal area$_{\text{H initiated}}$** <br> **[%]** |
|---|---|---|
| **3.00** | 72 | 28 |
| **2.00** | 74 | 26 |
| **1.50** | 74 | 26 |
| **1.00** | 82 | 18 |
| **0.75** | 83 | 17 |
| **0.50** | 74 | 26 |
| **0.25** | n.d. | n.d. |

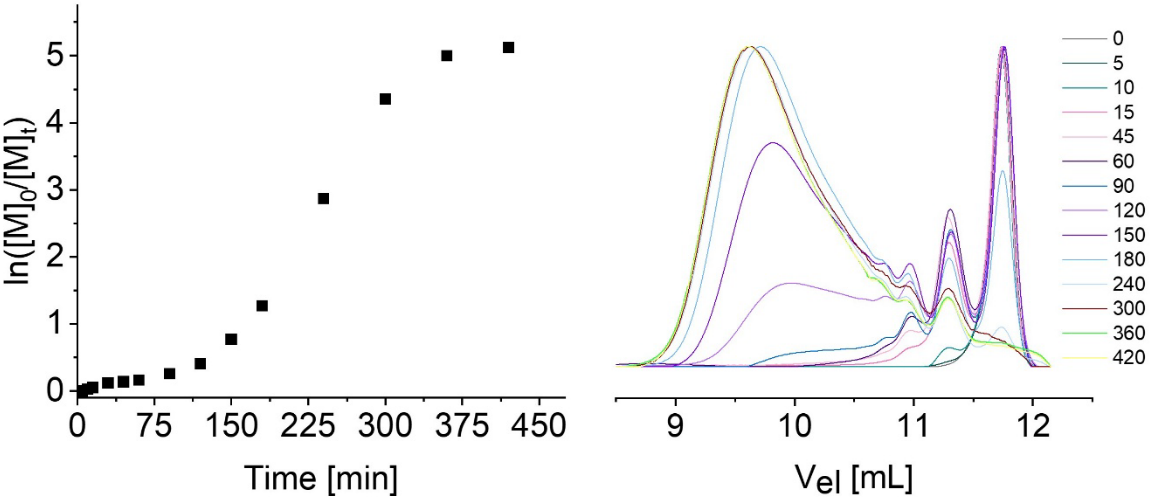

**Figure S15**: Kinetik investigation of the CROP of NonOx initiated by **3M**. ([M]$_0$/[I]$_0$ = 10, [M]$_0$ = 2 mol L$^{-1}$ in chlorobenzene, 135 °C). **A**: First-order kinetic plot. Conversion was determined *via* GC. **B**: Overlay of SEC elugrams (RID, PS calibration).

[M]/[I] = 10

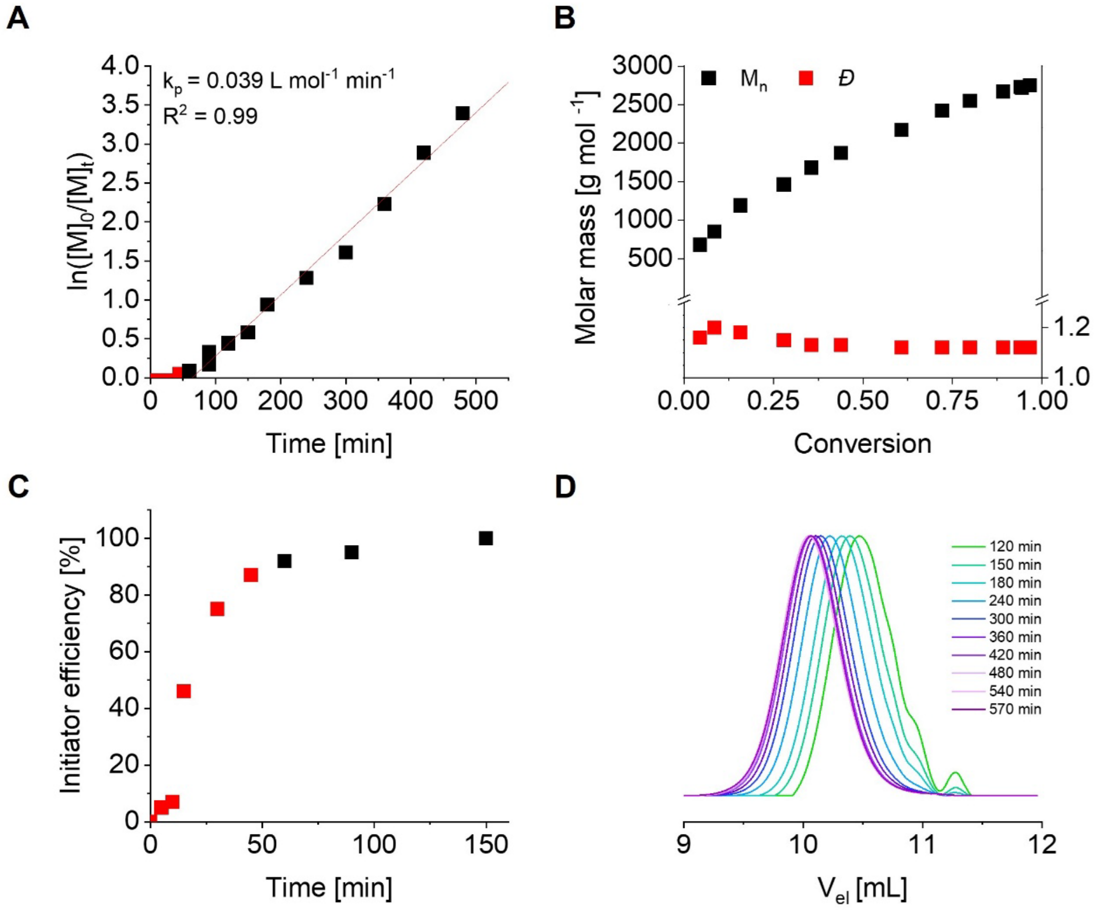

**Figure S16**: Kinetic investigation of the CROP of NonOx initiated by **3M** ($[M]_0/[I]_0 = 10$, $[M]_0 = 2$ mol L$^{-1}$ in $CH_3CN$, 85 °C). **A**: First-order kinetic plot according to $\ln([M]_0/[M]_t) = k_p \times [I]_0 \times t$. **B**: Evolution of the molar mass and dispersity with monomer conversion. Conversion was determined *via* GC. **C**: Initiator efficiency determined *via* $^1$H NMR spectroscopy. **D**: Overlay of SEC elugrams (RID, PS calibration).

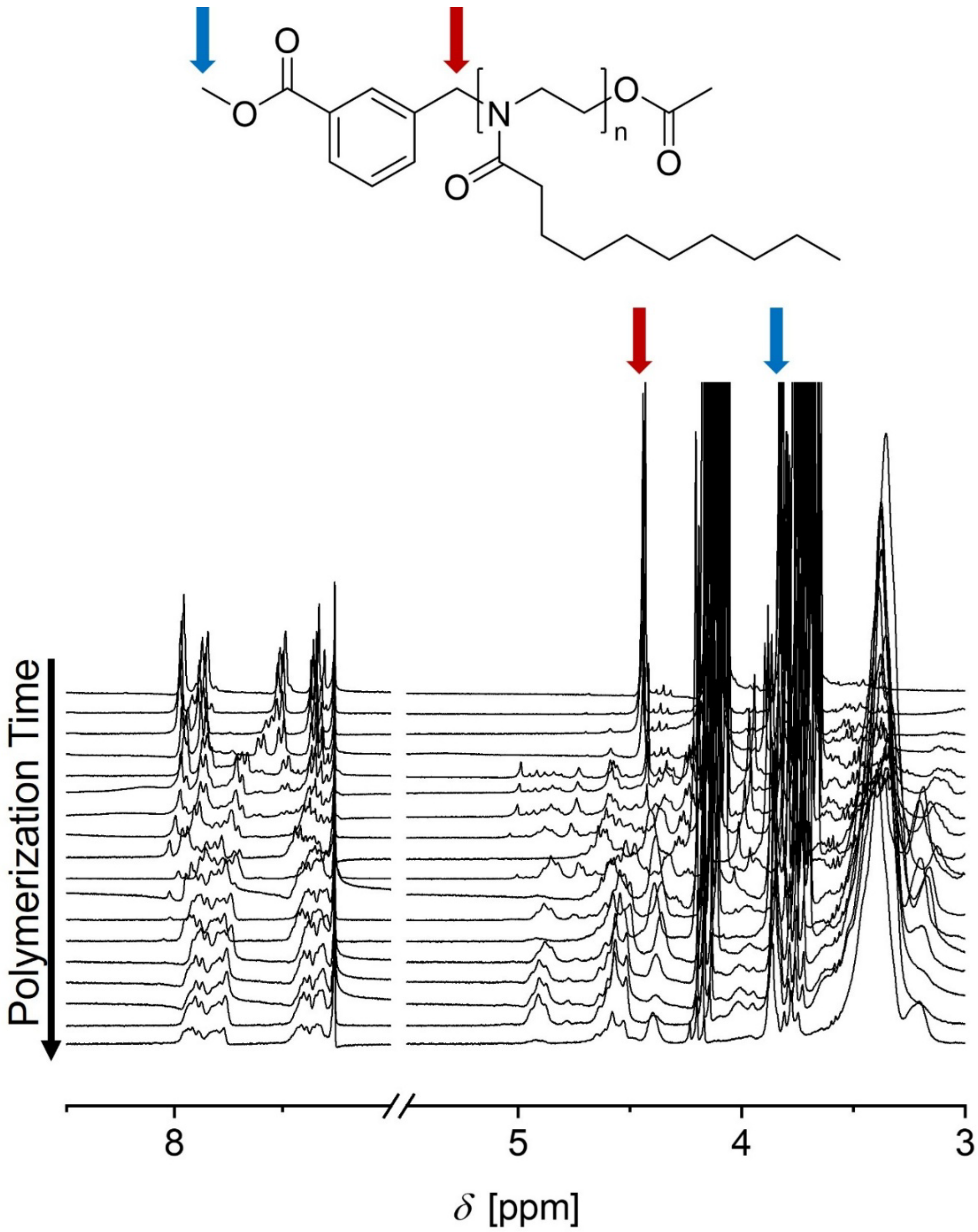

**Figure S17**: Overlay of $^1$H NMR spectra (300 MHz, $CDCl_3$) recorded during the kinetic studies of the CROP of NonOx initiated by **3M**. ($[M]_0/[I]_0 = 10$, $[M]_0 = 2$ mol $L^{-1}$ in $CH_3CN$, 85 °C). Arrows indicate the protons used to determine the initiation efficiency.

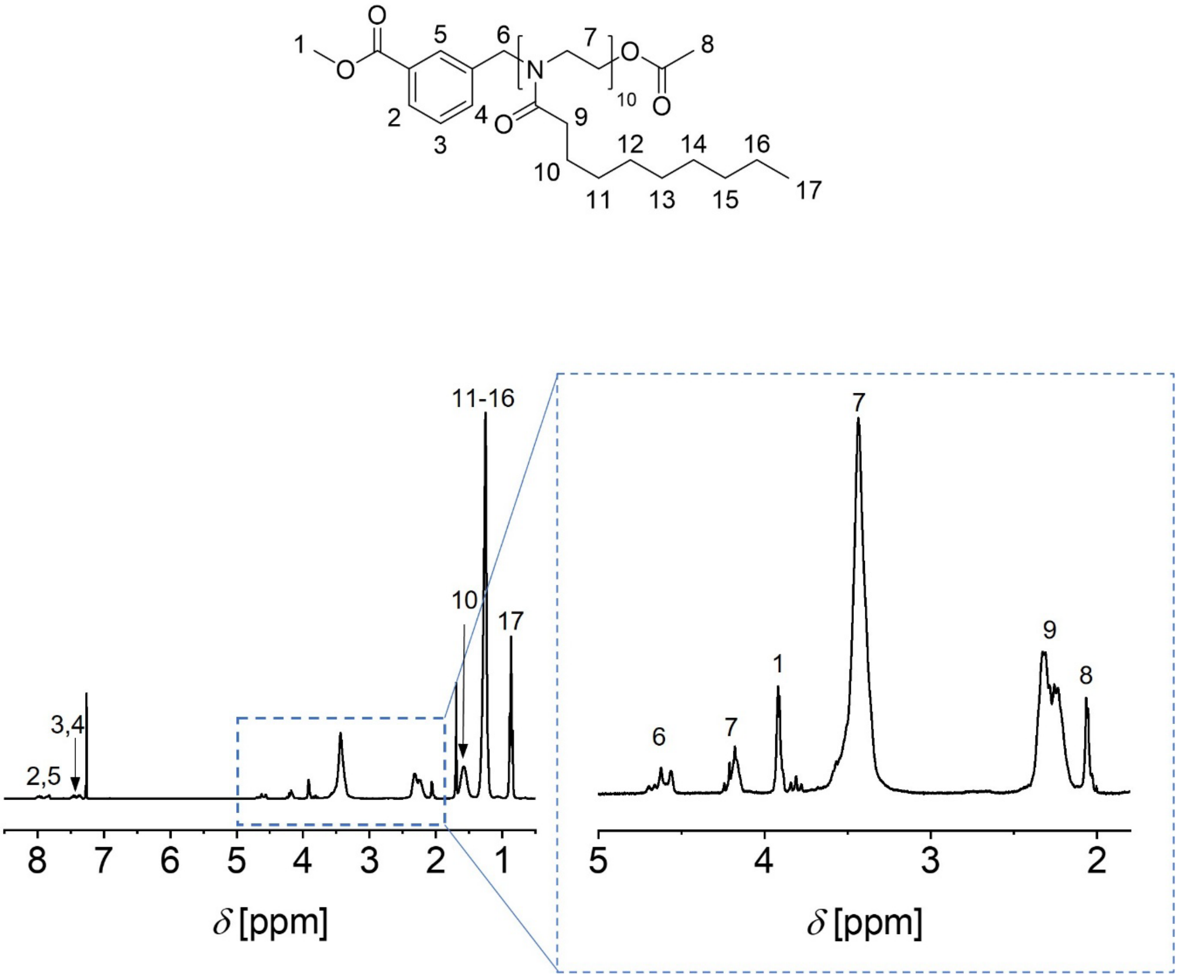

**Figure S18**: $^1$H NMR spectrum (300 MHz, $CDCl_3$) of **3M-NonOx$_{10}$-OAc** and assignments of the peaks to the schematic representation of the structure.

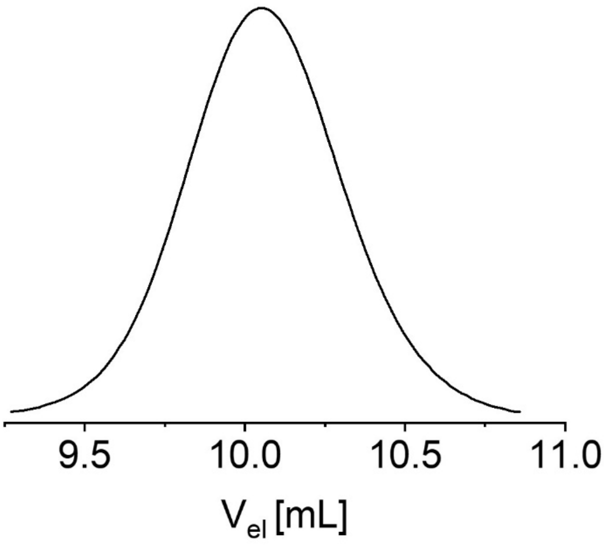

**Figure S19**: SEC elugram (RI detection) of **3M-NonOx$_{10}$-OAc**.

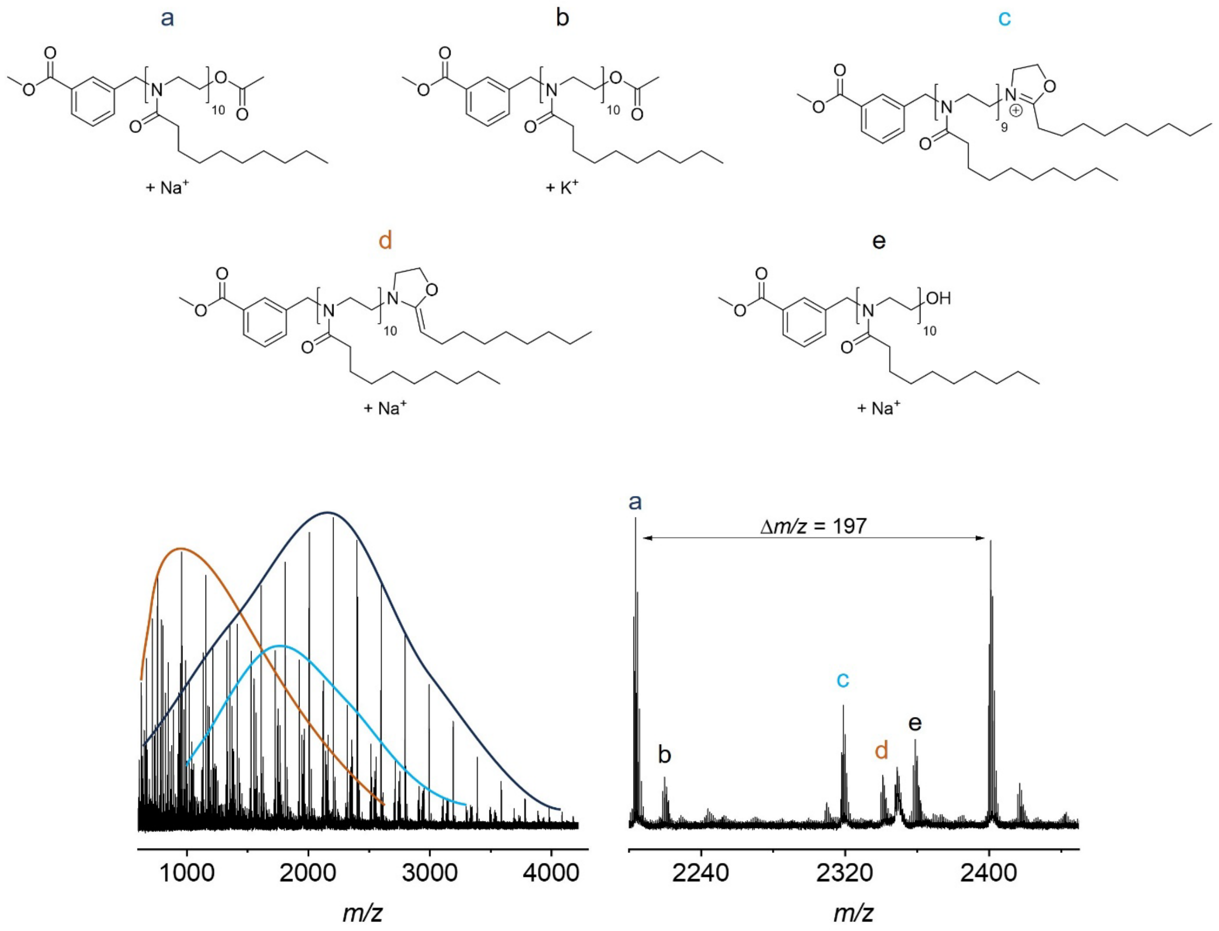

**Figure S20**: MALDI-TOF mass spectrum of **3M-NonOx$_{10}$-OAc**. Left: Full spectrum. Right: Zoom into the most abundant *m/z* region to display the NonOx repeating unit of Δ*m/z* = 197 and peak assignment.

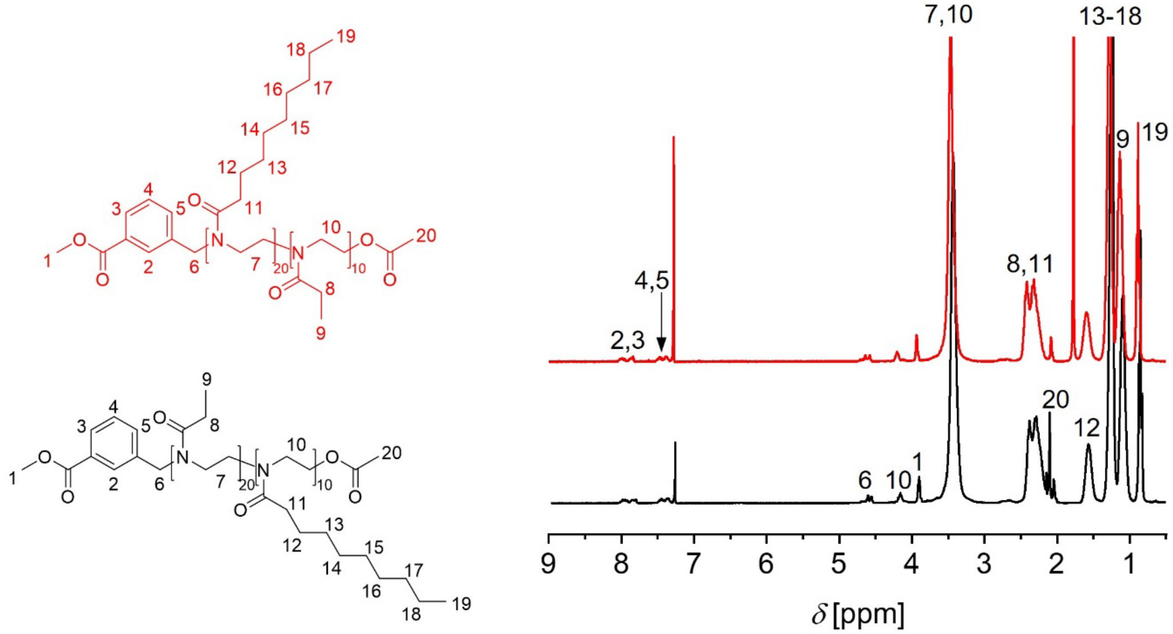

**Figure S21**: $^1$H NMR spectra (300 MHz, CDCl$_3$) of **3M-NonOx$_{10}$-*b*-EtOx$_{20}$-OAc** and **3M-EtOx$_{20}$-*b*-EtOx$_{20}$-OAc** and assignments of the peaks to the schematic representation of the structures. Signals 19 and 8, 11 were used to estimate the copolymer composition.

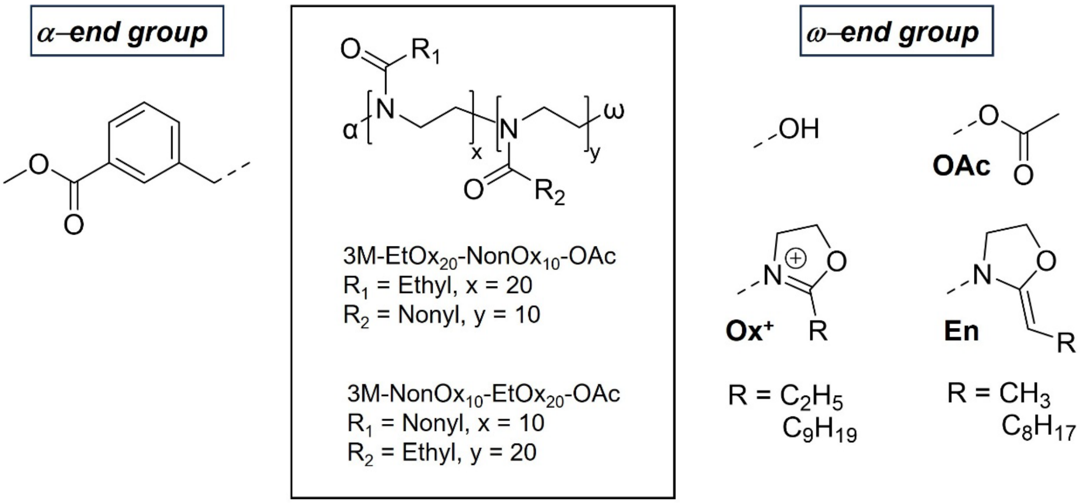

| | *m/z* | α | ω | Counter ion |
|---|---|---|---|---|
| a | 4184.21 | 3M<br>$C_9H_9O_2$ | OAc<br>$C_2H_3O_2$ | $Na^+$ |
| b | 4200.18 | 3M<br>$C_9H_9O_2$ | OAc<br>$C_2H_3O_2$ | $K^+$ |
| c | 4102.21 | 3M<br>$C_9H_9O_2$ | $Ox^+$<br>$C_5H_9NO/C_{12}H_{23}NO$ | - |
| d | 4223.26 or<br>4321.37 | 3M<br>$C_9H_9O_2$ | En<br>$C_5H_8NO/C_{12}H_{22}NO$ | $Na^+$ |
| e | 4142.20 | 3M<br>$C_9H_9O_2$ | OH | $Na^+$ |

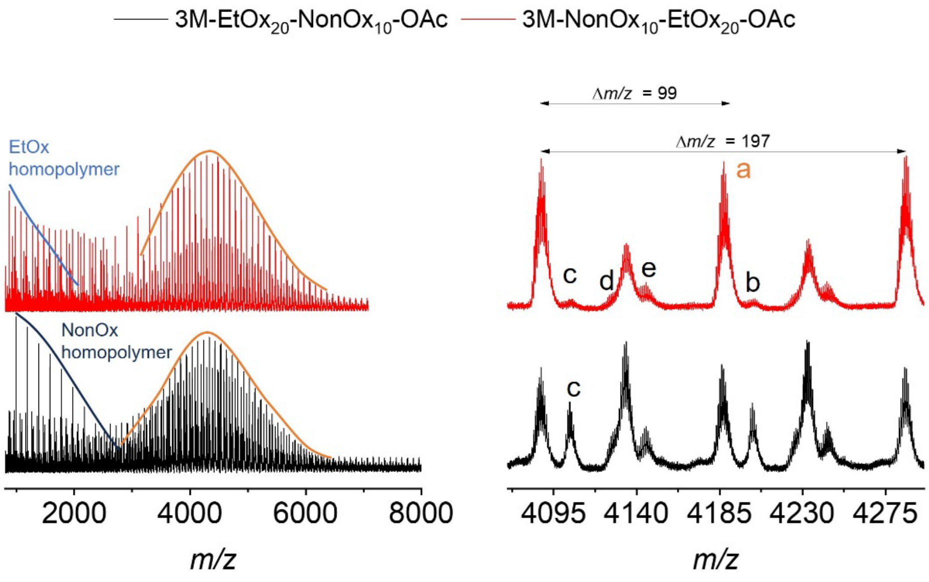

**Figure S22**: MALDI-TOF MS measurements of **3M-NonOx10-*b*-EtOx20-OAc** and **3M-EtOx20-*b*-NonOx10-OAc** (DCTB + NaTFA). Left: Full spectra. Right: Zoom into the most abundant *m/z* region and peak assignment.

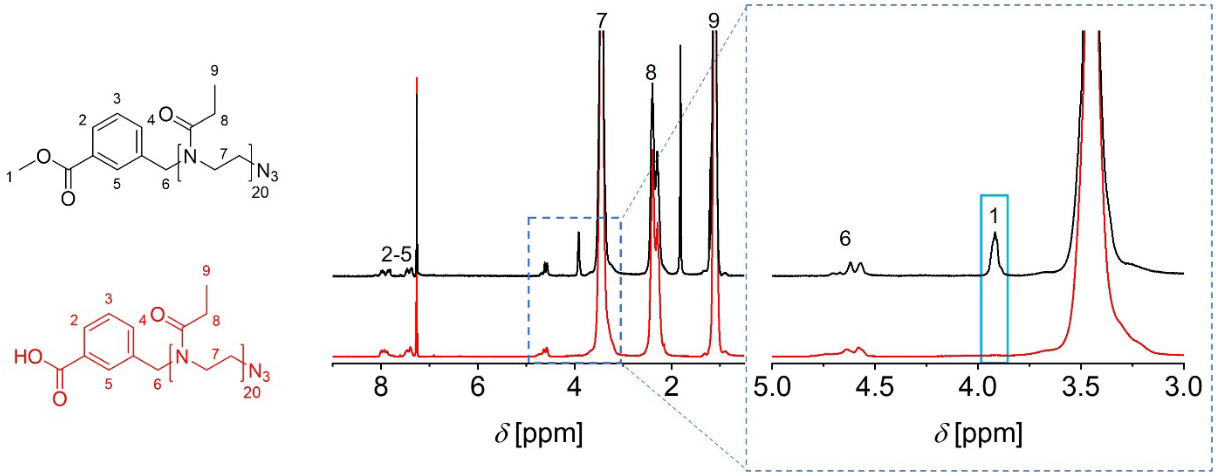

**Figure S23**: $^1$H NMR spectra (300 MHz, CDCl$_3$) of **3M-EtOx$_{20}$-N$_3$** and **3A-EtOx$_{20}$-N$_3$** and assignments of the peaks to the schematic representation of the structures. Right: Zoom into the area, where the disappearance of the peak of the methyl ester group is visible (blue box).

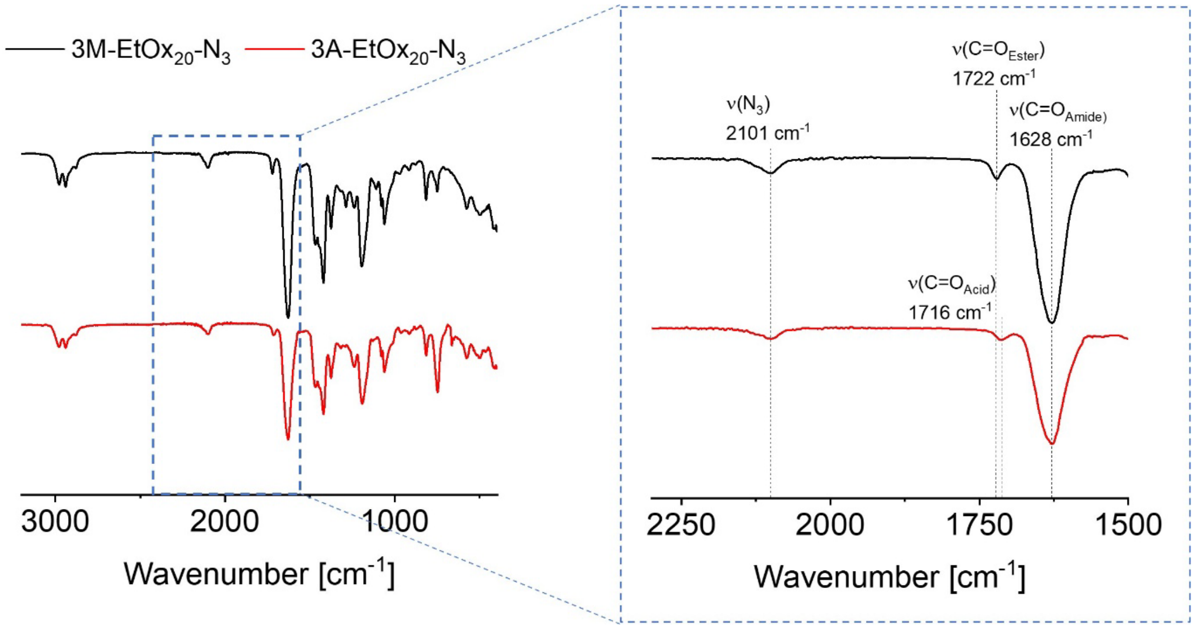

**Figure S24**: ATR-IR spectra of **3M-EtOx$_{20}$-N$_3$** and **3A-EtOx$_{20}$-N$_3$** and assignments of the characteristic vibrational bands.

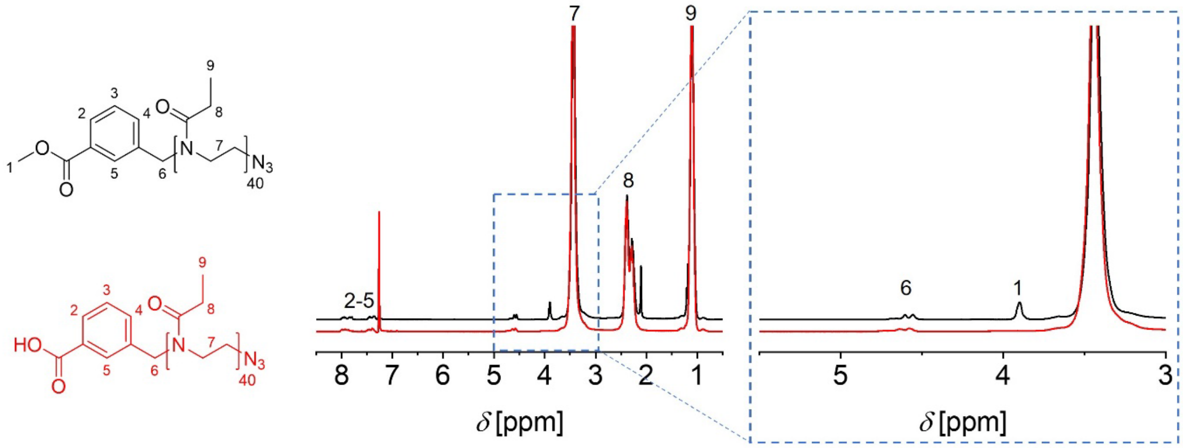

**Figure S25**: $^1$H NMR spectra (300 MHz, CDCl$_3$) of **3M-EtOx$_{40}$-N$_3$** and **3A-EtOx$_{40}$-N$_3$** and assignments of the peaks to the schematic representation of the structures.

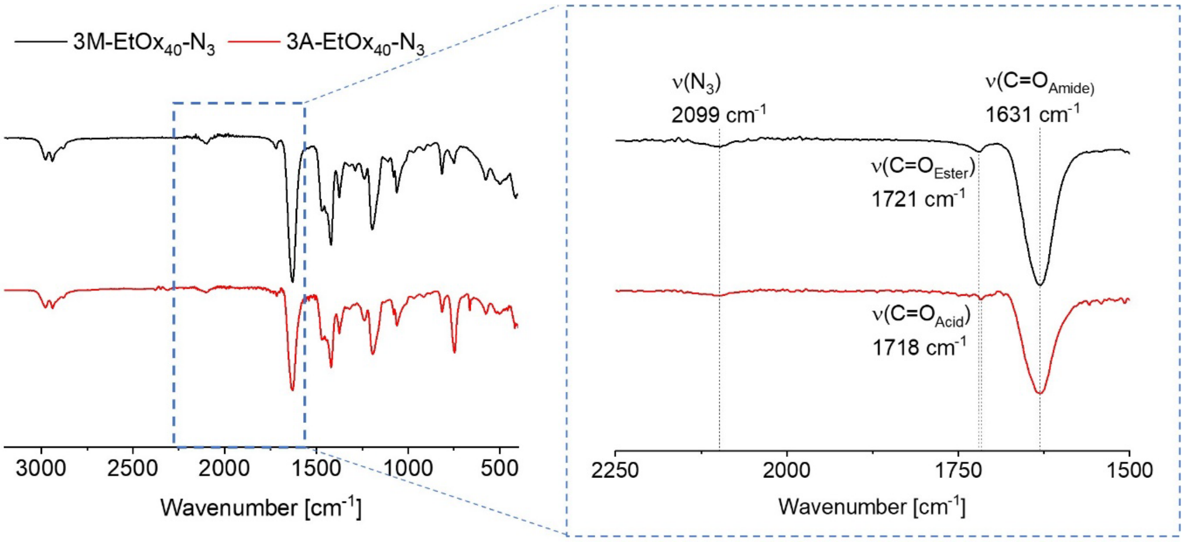

**Figure S26**: ATR-IR spectra of **3M-EtOx$_{40}$-N$_3$** and **3A-EtOx$_{40}$-N$_3$** and assignments of the characteristic vibrational bands.

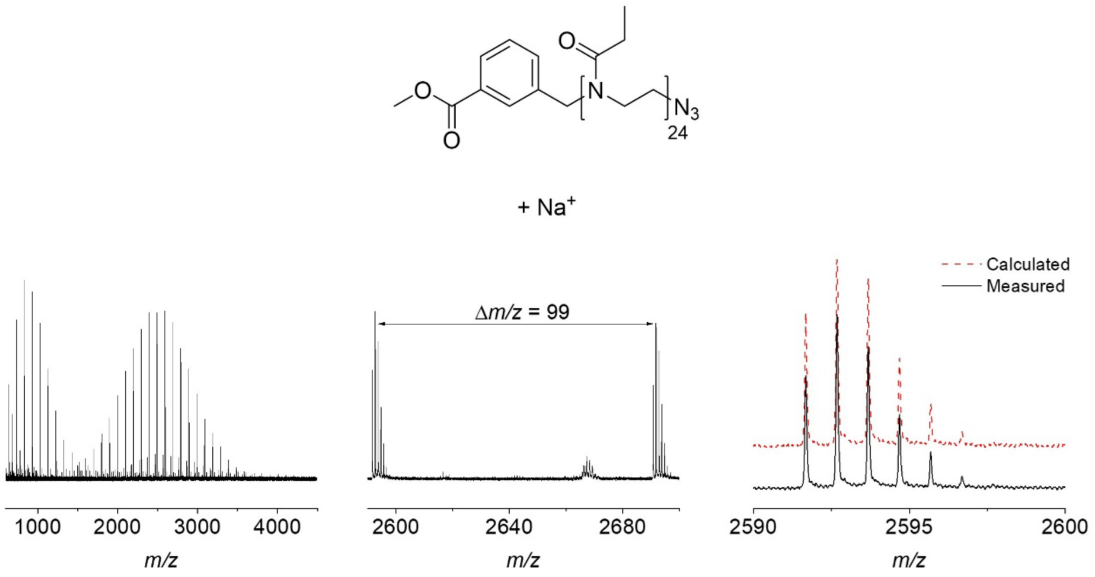

**Figure S27**: MALDI-TOF mass spectrum of **3M-EtOx$_{20}$-N$_3$**. Left: Full spectrum. Middle: Zoom into the most abundant *m/z* region to display the EtOx repeating unit of Δ*m/z* = 99. Right: Overlay of the measured and calculated isotopic pattern of the most abundant species ($[C_9H_9O_2(C_5H_9NO)_{24}N_3 + Na]^+$).

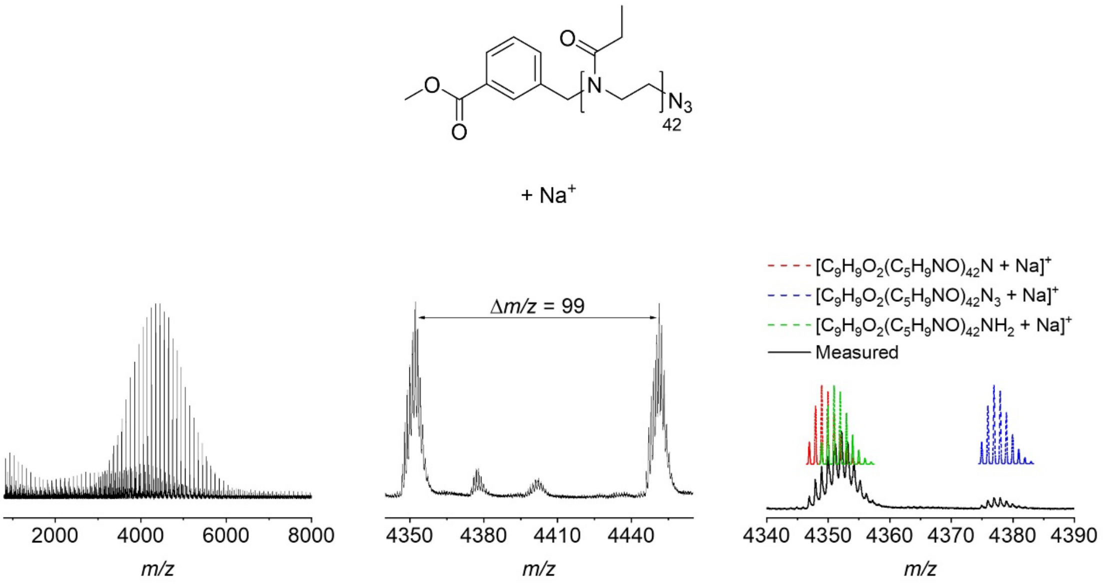

**Figure S28**: MALDI-TOF mass spectrum of **3M-EtOx$_{40}$-N$_3$**. Left: Full spectrum. Middle: Zoom into the most abundant *m/z* region to display the EtOx repeating unit of Δ*m/z* = 99. Right: Overlay of measured and calculated isotopic patterns for the assignment of detected *m/z* series.

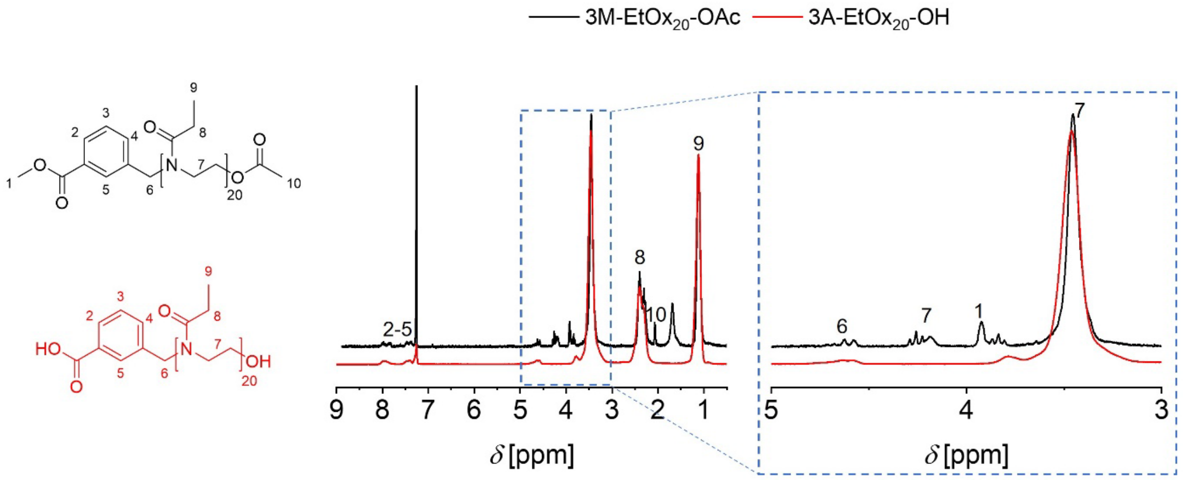

**Figure S29**: $^1$H NMR spectra (300 MHz, CDCl$_3$) of **3M-EtOx$_{20}$-OAc** and **3A-EtOx$_{20}$-OH** and assignments of the peaks to the schematic representation of the structures.

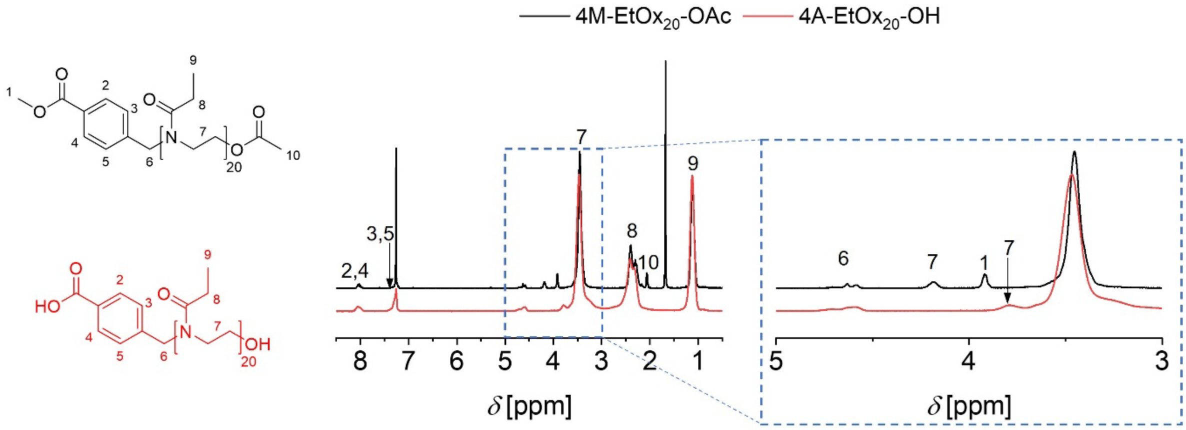

**Figure S30**: $^1$H NMR spectra (300 MHz, CDCl$_3$) of **4M-EtOx$_{20}$-OAc** and **4A-EtOx$_{20}$-OH** and assignments of the peaks to the schematic representation of the structures.

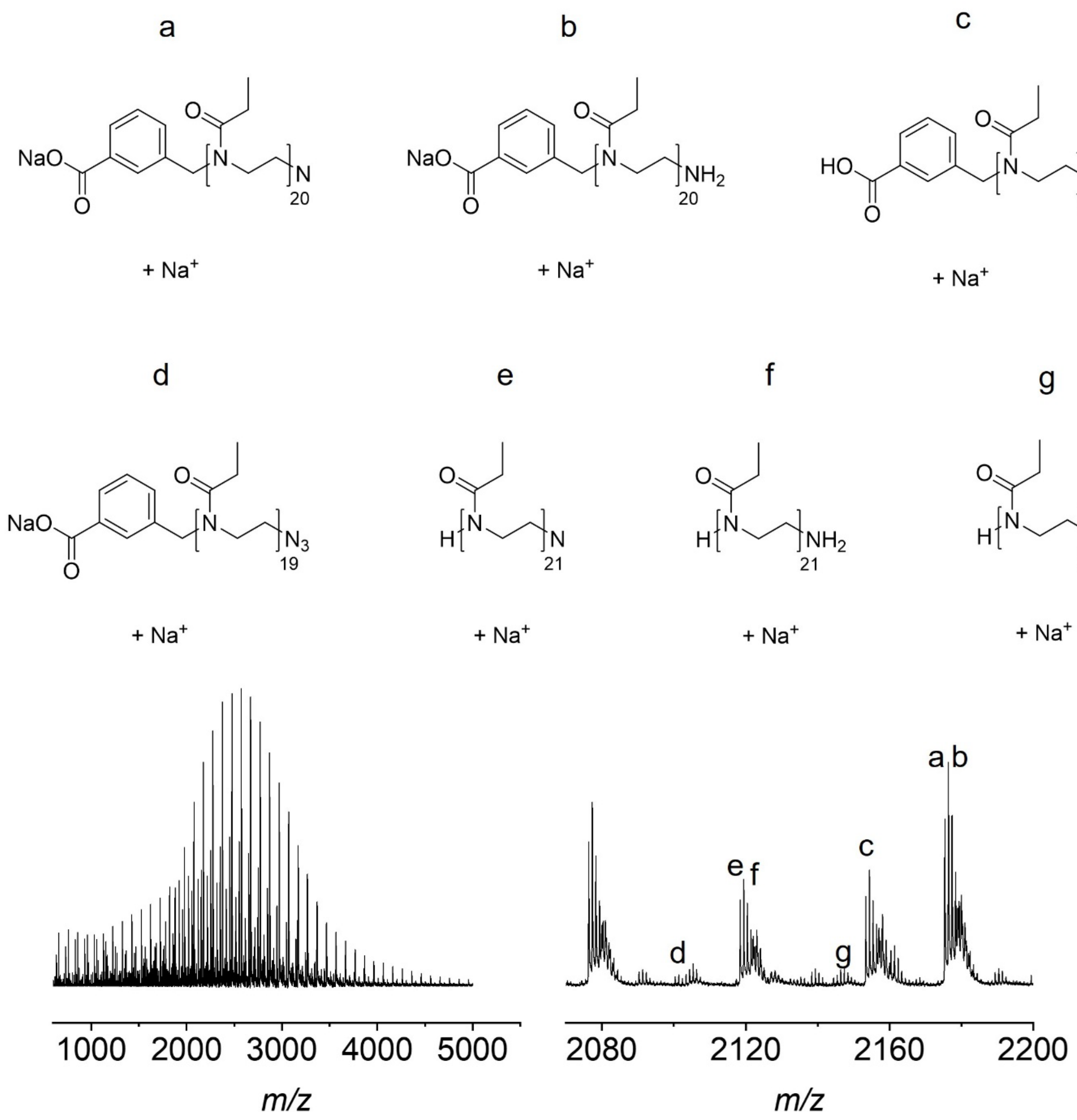

**Figure S31**: MALDI-TOF mass spectrum of **3A-EtOx$_{20}$-N$_3$**. Left: Full spectrum. Right: Assignment of detected *m/z* series.

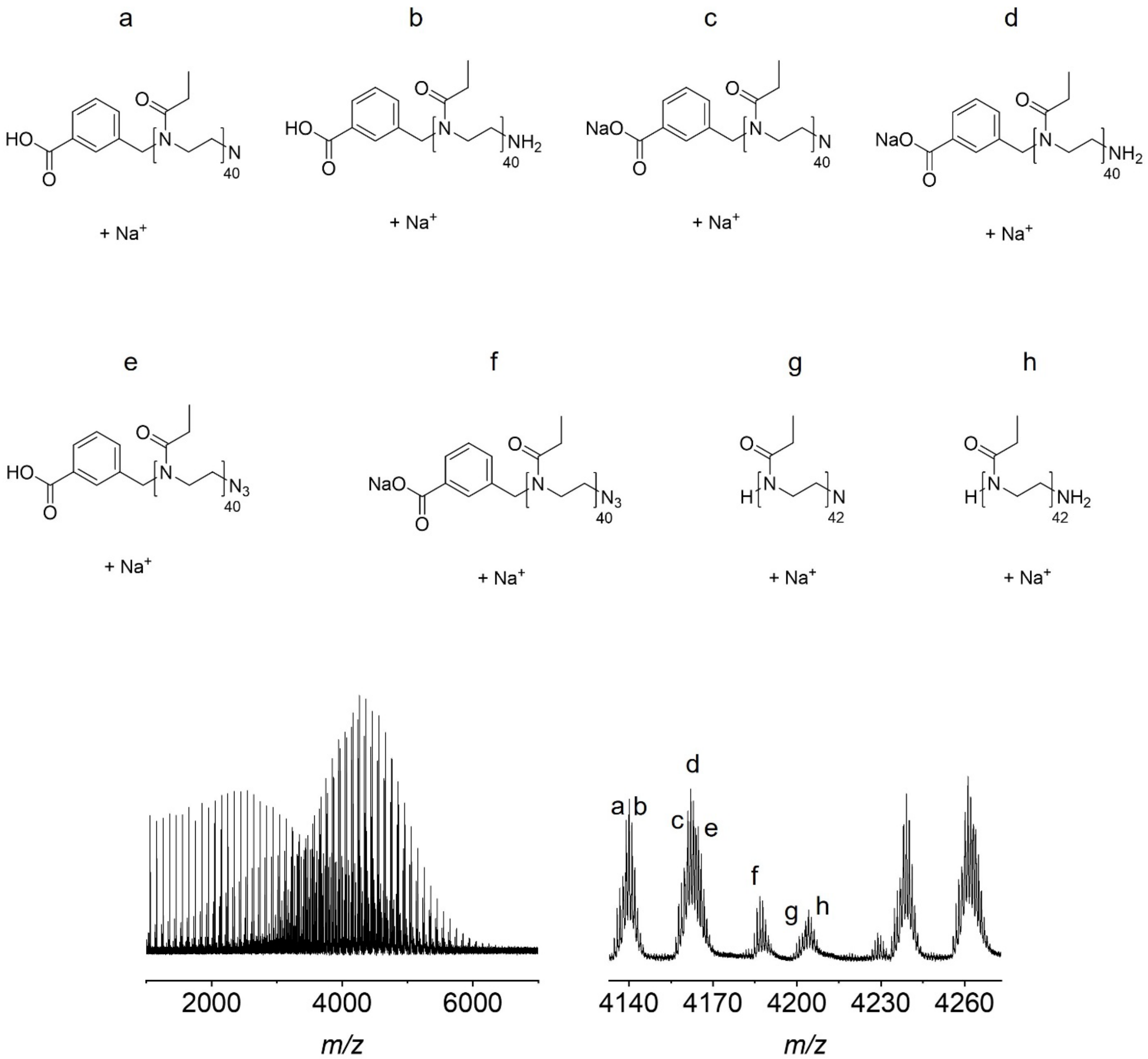

**Figure S32**: MALDI-TOF mass spectrum of **3A-EtOx$_{40}$-N$_3$**. Left: Full spectrum. Right: Assignment of detected *m/z* series.

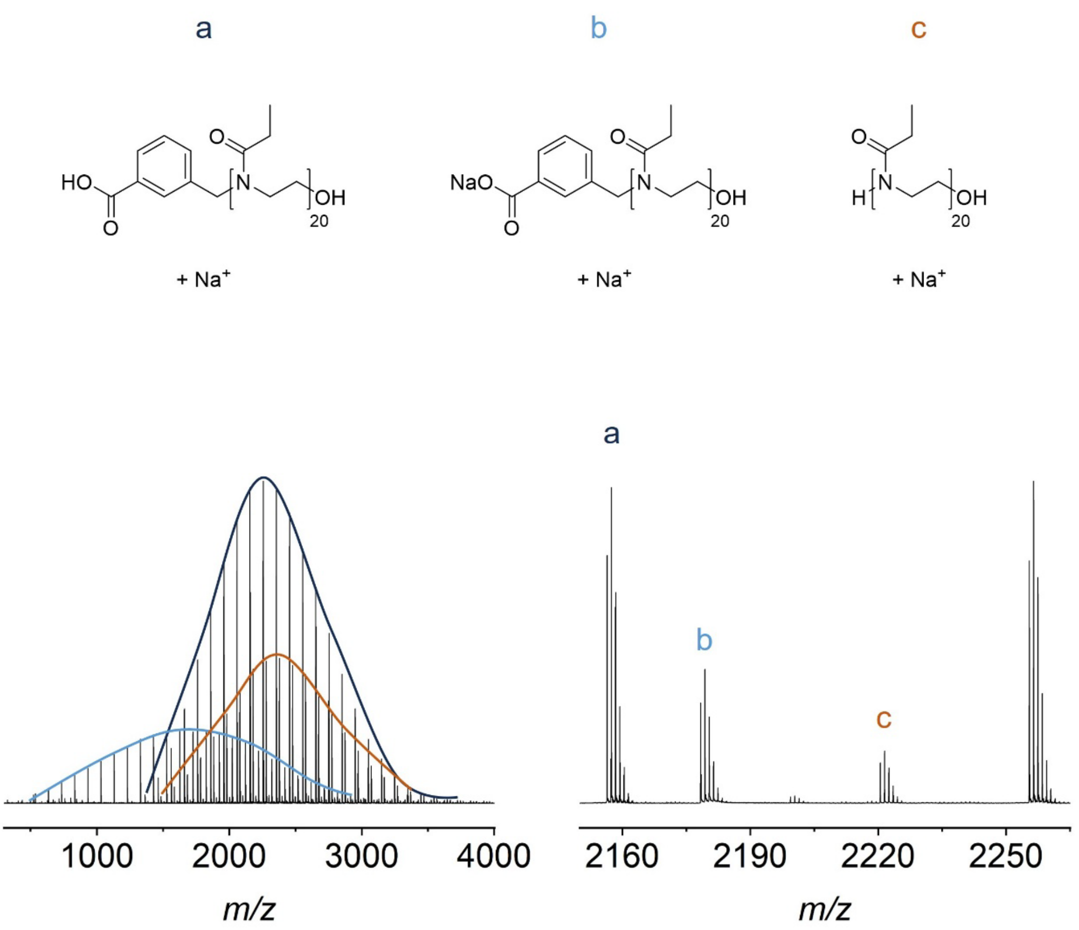

**Figure S33**: MALDI-TOF mass spectrum of **3A-EtOx$_{20}$-OH**. Left: Full spectrum. Right: Assignment of the detected *m/z* series.

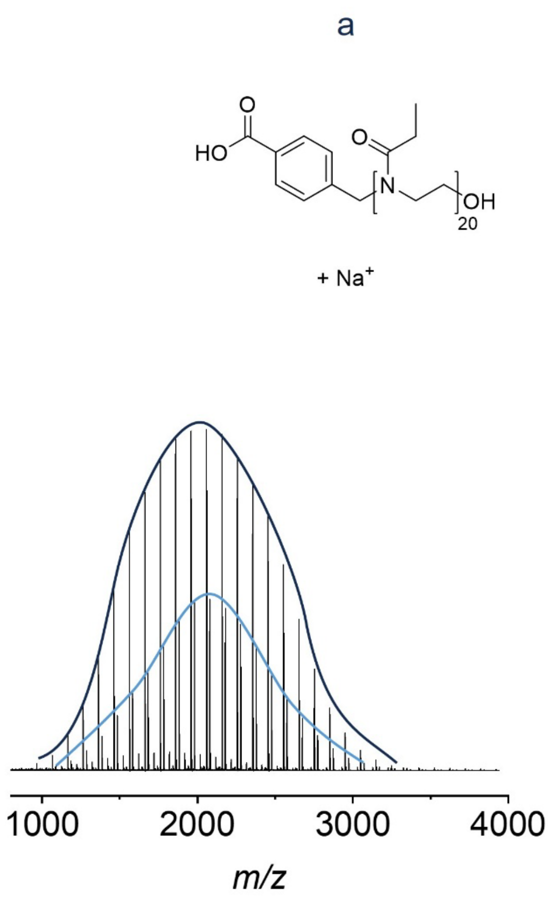

**Figure S34**: MALDI-TOF mass spectrum of **4A-EtOx$_{20}$-OH**. Left: Full spectrum. Right: Assignment of the detected *m/z* series.

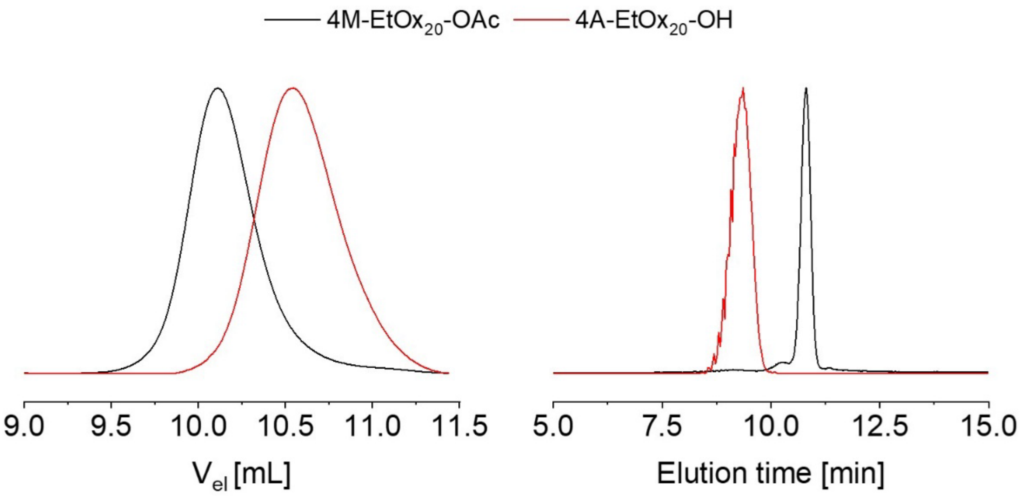

**Figure S35**: Chromatographic analysis of protected and deprotected PEtOx heterotelechelics obtained by initiation of CROP with **4M**. Left: SEC (RID). Right: HPLC (RP18 Chromolith column, water/acetonitrile gradient with 0.1% formic acid, ELSD).